9-2015

Reducing Conditions, Reactive Metals, and Their Interactions Can Explain Spatial Patterns of Surface Soil Carbon in a Humid Tropical Forest

Steven J. Hall
Iowa State University, stevenjh@iastate.edu

Whendee L. Silver
University of California - Berkeley

Reducing Conditions, Reactive Metals, and Their Iinteractions Can Explain Spatial Patterns of Surface Soil Carbon in a Humid Tropical Forest

Abstract
Humid tropical forests support large stocks of surface soil carbon (C) that exhibit high spatial variability over scales of meters to landscapes (km). Reactive minerals and organo-metal complexes are known to contribute to C accumulation in these ecosystems, although potential interactions with environmental factors such as oxygen (O2) availability have received much less attention. Reducing conditions can potentially contribute to C accumulation, yet anaerobic metabolic processes such as iron (Fe) reduction can also drive substantial C losses. We tested whether these factors could explain variation in soil C (0–10 and 10–20 cm depths) over multiple spatial scales in the Luquillo Experimental Forest, Puerto Rico, using reduced iron (Fe(II)) concentrations as an index of reducing conditions across sites differing in vegetation, topographic position, and/or climate. Fine root biomass and Fe(II) were the best overall correlates of site (n = 6) mean C concentrations and stocks from 0 to 20 cm depth (r = 0.99 and 0.98, respectively). Litterfall decreased as reducing conditions, total and dead fine root biomass, and soil C increased among sites, suggesting that decomposition rates rather than C inputs regulated soil C content at the landscape scale. Strong relationships between Fe(II) and dead fine root biomass suggest that reducing conditions suppressed particulate organic matter decomposition. The optimal mixed-effects regression model for individual soil samples (n = 149) showed that aluminum (Al) and Fe in citrate/ascorbate and oxalate extractions, Fe(II), fine root biomass, and interactions between Fe(II) and Al explained most of the variation in C concentrations (pseudo R2 = 0.82). The optimal model of C stocks was similar but did not include fine root biomass (pseudo R2 = 0.62). In these models, soil C concentrations and stocks increased with citrate/ascorbate-extractable Al and oxalate-extractable Fe. However, soil C decreased with citrate/ascorbate-extractable Fe, an index of Fe susceptible to anaerobic microbial reduction. At the site scale (n = 6), ratios of citrate/ascorbate to oxalate-extractable Fe consistently decreased across a landscape O2 gradient as C increased. We suggest that the impact of reducing conditions on organic matter decomposition and the presence of organo-metal complexes and C sorption by short-range order Fe and Al contribute to C accumulation, whereas the availability of an Fe pool to sustain anaerobic respiration in soil microsites partially attenuates soil C accumulation in these ecosystems.

Keywords
Dead Fine Root Biomass, Lowe Montane Forest, Live Fine Root, Decomposition Rate, Montane Site, Tropical Montane Forest, Root Productivity, Total Fine Root, Bulk Soil, Root Biomass Allocation, Ous Horizon, Bulk Density, Litter Decomposition Rate, Oxalate, Landscape Pattern

Disciplines
Ecology and Evolutionary Biology | Forest Sciences

Comments
This is a manuscript of an article in *Biogeochemistry* 125 (2015): 149, doi:10.1007/s10533-015-0120-5. Posted with permission.

Reducing conditions, reactive metals, and their interactions can explain spatial patterns of surface soil carbon in a humid tropical forest

Steven J. Hall*, Whendee L. Silver

Department of Environmental Science, Policy, and Management
University of California-Berkeley
130 Mulford Hall, UC Berkeley, Berkeley, CA 94720

New address and contact information for corresponding author*:

Department of Ecology, Evolution, and Organismal Biology, Iowa State University

stevenjh@iastate.edu

608-886-6752

251 Bessey Hall, Iowa State University, Ames, IA 50011

Abstract

Humid tropical forests support large stocks of surface soil carbon (C) that exhibit high spatial variability over scales of meters to landscapes (km). Reactive minerals and organo-metal complexes are known to contribute to C accumulation in these ecosystems, although potential interactions with environmental factors such as oxygen (O_2) availability have received much less attention. Reducing conditions can potentially contribute to C accumulation, yet anaerobic metabolic processes such as iron (Fe) reduction can also drive substantial C losses. We tested whether these factors could explain variation in soil C (0 – 10 and 10 – 20 cm depths) over multiple spatial scales in the Luquillo Experimental Forest, Puerto Rico, using reduced iron (Fe(II)) concentrations as an index of reducing conditions across sites differing in vegetation, topographic position, and/or climate. Fine root biomass and Fe(II) were the best overall correlates of site (n = 6) mean C concentrations and stocks from 0 to 20 cm depth (r = 0.99 and 0.98, respectively). Litterfall decreased as reducing conditions, total and dead fine root biomass, and soil C increased among sites, suggesting that decomposition rates rather than C inputs regulated soil C content at the landscape scale. Strong relationships between Fe(II) and dead fine root biomass suggest that reducing conditions suppressed particulate organic matter decomposition. The optimal mixed-effects regression model for individual soil samples (n = 149) showed that aluminum (Al) and Fe in citrate/ascorbate and oxalate extractions, Fe(II), fine root biomass, and interactions between Fe(II) and Al explained most of the variation in C concentrations (pseudo $R^2 = 0.82$). The optimal model of C stocks was similar but did not include fine root biomass (pseudo $R^2 = 0.62$). In these models, soil C concentrations and stocks

increased with citrate/ascorbate-extractable Al and oxalate-extractable Fe. However, soil C decreased with citrate/ascorbate-extractable Fe, an index of Fe susceptible to anaerobic microbial reduction. At the site scale (n = 6), ratios of citrate/ascorbate to oxalate-extractable Fe consistently decreased across a landscape O_2 gradient as C increased. We suggest that the impact of reducing conditions on organic matter decomposition and the presence of organo-metal complexes and C sorption by short-range order Fe and Al contribute to C accumulation, whereas the availability of an Fe pool to sustain anaerobic respiration in soil microsites partially attenuates soil C accumulation in these ecosystems.

Keywords: humid tropical forest, iron reduction, Luquillo Experimental Forest, poorly-crystalline minerals, redox, root biomass, soil carbon, soil oxygen

1. Introduction

Identifying the mechanisms underlying the accumulation and distribution of soil C in humid tropical forests represents an important challenge given their large soil C stock (~ 500 Pg), rapid decomposition rates, and potentially large feedbacks to global climate change (Jobbagy and Jackson 2000; Malhi and Grace 2000; Parton et al. 2007). Numerous studies have demonstrated the importance of short-range order and monomeric Al and Fe in protecting organic matter from microbial decomposition due to mineral sorption and the precipitation of organo-metal complexes (e.g. Baldock and Skjemstad 2000; Kaiser and Guggenberger 2000; Wagai and Mayer 2007). Accordingly, increasing concentrations of short-range order minerals or poorly-crystalline Fe and Al measured in chemical extractions have often correlated with decreased decomposition rates and increased C concentrations across a broad spectrum of temperate and tropical ecosystems (Torn et al. 1997; Kleber et al. 2005; Bruun et al. 2010;

65 Kramer et al. 2012). In wet ecosystems characteristic of the humid tropics, variation in soil O_2
66 availability and the consequent prevalence of hypoxia or reducing conditions can also
67 significantly impact surface soil C cycling (Silver et al. 1999; Schuur 2001; Schuur et al. 2001;
68 Liptzin et al. 2011), but these mechanisms have received little attention in comparison with
69 short-range order minerals and metals. Importantly, soil O_2 concentrations are closely linked
70 with climate via precipitation and temperature patterns at landscape scales (Silver et al. 1999;
71 Silver et al. 2013), thus providing a potential mechanistic linkage between spatial and temporal
72 variation in climate and soil C stocks that could be included in process-based models. Here, we
73 tested whether multiple indices of reactive Fe and Al, reducing conditions, and their interactions
74 could explain the distribution of surface soil C (0 – 10 and 10 – 20 cm depth increments) over
75 coarse and fine spatial scales across a humid tropical forest landscape. We define reactive Fe and
76 Al pools operationally in terms of multiple chemical extractions used in this study, which are
77 explained in detail in the Methods.

78 Humid tropical forests often experience a combination of high precipitation, temperature,
79 and soil respiration that generates periodic oxygen (O_2) limitation in surface soils at scales of
80 microsites to entire soil profiles (Silver et al. 1999; Schuur et al. 2001; Cleveland et al. 2010;
81 Liptzin et al. 2011; Silver et al. 2013; Hall et al. 2013). Soil O_2 availability and the prevalence of
82 reducing microsites vary with precipitation, soil moisture, and soil texture and structure, which
83 control diffusive O_2 supply to the soil profile, as well as heterotrophic and autotrophic
84 respiration, which control rates of O_2 consumption. Anaerobic conditions are well known to
85 constrain organic matter decomposition in flooded wetland ecosystems (Ponnamperuma 1972),
86 but the potential influence of O_2 limitation on C accumulation in terrestrial soils has received less
87 attention. Soil C stocks increased monotonically with decreasing redox potential across a

precipitation gradient in Hawaii even as plant productivity declined, suggesting that reducing conditions promoted soil C accumulation at the landscape scale (Schuur et al. 2001). Concentrations of short-range order minerals declined with increasing precipitation along the same gradient, implying that anaerobic constraints on decomposition as opposed to organo-mineral interactions were primarily responsible for increased C accumulation (ibid.). Soil C concentrations and stocks increased with elevation in New Guinean and Puerto Rican humid tropical forests, although relationships with short-range order minerals and reducing conditions were not quantified (McGroddy and Silver 2000; Dieleman et al. 2013).

Understanding the potentially nuanced interactions between O_2 availability and reactive metals could provide additional insight into spatial patterns of C in humid tropical forest soils. In particular, impacts of reducing conditions on soil C storage may depend on multiple additional factors related to Fe and Al speciation and concentrations. Previous research examining organo-mineral interactions in upland soils has largely emphasized the capacity of Fe oxides to protect C from decomposition via sorption and complexation (e.g. Kleber et al. 2005; Wagai and Mayer 2007), with less emphasis on their capacity to facilitate C loss during anaerobic respiration (Peretyazhko and Sposito 2005). Although the anaerobic metabolic process of dissimilatory Fe reduction has primarily been studied in submerged sediments, it has been shown to sustain high rates of microbial respiration in surface horizons of terrestrial humid tropical soils, where densities of Fe reducing bacteria can exceed those of submerged sediments (Chacón et al. 2006; Thompson et al. 2006; Dubinsky et al. 2010, DeAngelis et al. 2010). Rates of CO_2 production from Fe reduction can be highly significant: anaerobic respiration rates from a tropical Ultisol measured 70 – 100 % of aerobic controls over short-term incubations (McNicol and Silver 2014). Although short-range order Fe oxides are often abundant in humid tropical soils, they can

111 eventually be depleted by reduction and leaching over pedogenic timescales (Thompson et al.
112 2011), which could ultimately limit the overall importance of Fe reduction and contribute to soil
113 C accumulation.

114 To evaluate relationships between reducing conditions, reactive minerals/metals, and soil
115 C, we collected 149 soil samples from six sites encompassing variation in soil O_2 dynamics
116 driven by topography and climate. At landscape scales, biological factors affecting C inputs
117 likely co-vary with physical and geochemical factors affecting C accumulation. Therefore, we
118 also report litterfall productivity (NPP) at the site scale, and report fine root biomass at the scale
119 of individual soil samples. Although fine root biomass is not an effective proxy for root
120 productivity, it can provide an index of the decomposition rates of particulate organic matter,
121 relative patterns of belowground C allocation, and/or nutrient limitation (Vogt et al. 1996;
122 Ostertag 2001; Espeleta and Clark 2007). These factors are important given that fine roots
123 represent a dominant source of soil C (Rasse et al. 2005). Furthermore, fine roots can be assayed
124 at the same fine spatial scales (cm) as soil chemical constituents and C concentrations, yet few
125 studies of fine roots have been combined with high-resolution measurements of soil C within
126 ecosystems (Vogt et al. 1996). The majority of samples (n = 119) in this study were collected
127 from four replicate catenas in a lower montane forest that experienced similar climate, and also
128 from three other montane sites (n = 30) characterized by higher rainfall and slightly lower
129 temperatures. Previous work showed that mineral-associated as opposed to particulate C is
130 dominant in the lower montane sites and at least one of the montane sites, accounting for 75 – 90
131 % of total C in surface horizons on a mass basis (Cusack et al., 2011; Hall et al., 2015).
132 However, particulate C is increasingly important in the two highest-elevation sites (McGroddy
133 and Silver 2000). In particular, we sought to address the relative importance of reducing

conditions, fine roots, and multiple reactive Al and Fe fractions as potential mechanisms associated with C accumulation.

2. Methods

2.1 Site description

We sampled soils from the Luquillo Experimental Forest, Puerto Rico, an NSF-funded Long Term Ecological Research and Critical Zone Observatory site (Table 1). We intensively sampled four ridge/slope/valley catenas in a lower montane (200 – 300 masl) forest in the Bisley watersheds, and we sampled ridge positions in three higher-elevation montane forests at 610, 740, and 940 masl, respectively. We emphasize that because we sampled four separate catenas in the lower montane forest, our data can be considered broadly representative of that forest type. For the montane forest sites, our data are representative of the selected sites (due to random selection of sampling plots), but not the forest types as a whole due to the lack of site replication. Rather, sites were selected because of their position on a climate/soil O_2 gradient, detailed below (Silver et al. 1999; Silver et al. 2013).

The Bisley watershed is described locally as a tabonuco forest after the dominant species, *Dacryodes excelsa* Vahl, and supports 127 shrub and tree species (Chinea et al. 1994). Together, *D. excelsa*, *Sloanea berteriana* Choisy ex. DC, and *Prestoea acuminata* (Willd.) H.E. Moore var. montana (Graham) A. Hend. & G. Galeano, known locally as sierra palm, comprised approximately 60 % of total aboveground biomass (Scatena and Lugo, 1995). Species composition varies with topographic position, and Heartsill-Scalley et al. (2010) provide a detailed description of spatial and temporal vegetation trends in this forest. Aboveground

biomass also varied strongly with topographic position, decreasing from 360 ± 60 Mg Ha^{-1} on ridges to 190 ± 30 and 120 ± 60 Mg Ha^{-1} in valleys (Scatena and Lugo 1995). However, litterfall NPP was statistically similar among topographic positions (US Forest Service International Institute for Tropical Forestry, unpublished data). Understory vegetation was sparse in all sites sampled here.

The forested site at 610 m was dominated by sierra palm, the 740 m site by palo colorado (*Cyrilla racemiflora* L.), and the 940 m site supported a cloud forest dominated by *Tabebuia rigida* Urb. The latter species typically comprises more than 50 % of tree basal area in these communities, which are locally described and referred to here as "elfin forests" due to their stunted vegetation canopy (Weaver et al. 1986). The frequent presence of fog, low soil O_2 availability, and high winds likely constrain NPP in the elfin forest relative to the other sites sampled here. Aboveground litterfall was greatest in the lower montane forest, intermediate in the sierra palm and palo colorado sites, and lowest in the elfin forest site (Table 1). We note that litterfall measurements reflect means from multiple litter baskets distributed within the sites, and thus could not be included in mixed-effects models of soil C at the finer spatial scales of individual soil samples. Litter decomposition rates are extremely rapid in the lower montane forest, with mean residence times of 0.8 and 0.9 y for leaves and roots, respectively (Cusack et al. 2009). Litter decomposition rates were lower in the palo colorado and elfin forests, where a separate study measured mean litter residence times of 1.1 and 2.7 y, respectively (DeAngelis et al. 2013).

Soils in these forests are largely derived from andesitic to basaltic volcaniclastic sedimentary rocks, with a likely contribution from quartz diorite in the palo colorado site. In the

177 lower montane forest, soils on stable ridges are dominantly Ultisols (Typic Haplohumults),
178 slopes are Oxisols (Inceptic and Aquic Hapludox), and valleys are Inceptisols (Typic Eutrudepts;
179 Soil Survey Staff 2002). In the montane sites, palm forest soils are Inceptisols (Aquandic
180 Humaquepts), and palo colorado and elfin forest soils are Oxisols (Humic Haplaquox). The
181 lower montane forest received a long-term mean annual precipitation of 3800 mm yr^{-1}, which
182 varied between 2600 – 5800 mm yr^{-1} from 1989 to 2011
183 (http://criticalzone.org/luquillo/data/dataset/2403/). Mean annual precipitation increases with
184 elevation in the Luquillo Mountains and measures approximately 4500 mm yr^{-1} in the elfin forest
185 (McDowell et al. 2012), although additional inputs from horizontal precipitation, fog, and cloud-
186 water inputs are important but difficult to quantify. Precipitation is relatively aseasonal, as even
187 the driest months (January and February) receive mean rainfall of 190 and 180 mm, respectively.
188 Mean annual temperature measures 24 °C in the lower montane forest and decreases with
189 elevation to 20 °C in the elfin forest with little intra-annual variability (McDowell et al. 2012).
190 Precipitation and temperature in the sierra palm and palo colorado sites are intermediate between
191 the elfin and the lower montane sites. These sites are frequently impacted by hurricanes,
192 although storms do not have a discernable short-term impact on soil C as evidenced by repeated
193 measurements over a decade that included multiple hurricanes (Teh et al. 2009).

194 These forested sites represent a gradient in soil O_2 concentrations, measured in gas
195 equilibration chambers (10 cm depth) over multiple years (Silver et al. 1999; Silver et al. 2013).
196 Mean soil O_2 decreased from ridges to slopes to riparian valleys in the lower montane forest (19,
197 16, and 11 % O_2, respectively, with the riparian valleys experiencing frequent low O_2 events (< 3
198 %). Mean O_2 decreased further as elevation increased from the sierra palm to palo colorado to
199 elfin forest sites, measuring approximately 10, 9, and 8 % O_2, respectively; similarly, these sites

were characterized by frequent periods of O_2 concentrations < 3 %. Elevated methane concentrations indicate the presence of anaerobic microsites (Silver et al. 1999). Because Fe oxides represent the most abundant anaerobic terminal electron acceptor in these soils (Hall et al. 2013), we used measurements of Fe(II) (described below) to provide an index of reducing conditions at the scale of individual soil samples. Previous studies have often used redox potential measurements (Eh) to characterize reducing conditions in soil microsites. However, Eh measurements are highly spatially variable and are difficult to compare among soils (Christensen et al. 2000). In contrast, measurements of Fe(II) and Fe(III) in soil extractions are quantitative, chemically meaningful, and integrate a defined soil volume.

2.2 Soil sampling and analysis

In the lower montane forest, we sampled four catenas in June 2011 that each consisted of a ridge, slope, and riparian valley. We randomly located five plots (0.25 m^2) in each topographic zone in each catena, along 50 m linear transects at 5 – 10 m intervals. We similarly sampled transects in ridge positions of the montane forest sites (one transect per site) in February 2012, yielding a total of 119 samples from the lower montane forest (rocks prevented collection of one sample) and 30 samples from the montane forest sites (total n = 149). In each plot, we collected four replicate 6-cm diameter soil cores (volume = 283 cm^3) at depths of 0 – 10 cm and 10 – 20 cm, where root biomass and organic matter are most abundant in these forests (Silver and Vogt 1993, Silver et al. 1994). Recognizable surface litter (Oi horizon material) was carefully removed where present prior to soil sampling. Accumulated surface litter tends to be sparse and discontinuous in the lower montane sites and slightly greater in the montane sites, and represents < 5 % of total soil C to 20 cm (Johnson et al. 2015). The 0 – 10 cm increment corresponded closely with the depth of the A horizon in most plots, whereas the 10 – 20 cm increment

223 typically represented the upper portion of a Bt horizon. Representative soil pits in a lower
224 montane ridge, slope, and valley had A horizons at depths of 0 – 10, 0 – 9, and 0 – 10 cm, and
225 B1 horizons at depths of 10 – 22, 9 – 25, and 10 – 20 cm, respectively. Soil depth did not exceed
226 20 cm in some riparian valley plots due to the presence of buried boulders. Thus, we sampled
227 common depth intervals present in all plots. We note that 0 – 10 cm samples from the palm
228 forest had extremely low bulk density, although samples were clearly differentiated from surface
229 litter by the presence of mineral soil aggregation. In the elfin forest, we avoided sampling soils
230 immediately adjacent to woody superficial roots, which are common in this forest type.

231 We used four separate soil extraction protocols that provide different operationally
232 defined indices of reactive Fe and Al, described below and in Table 2. Wagai et al. (2011) further
233 discuss several of these extraction methods. Two cores from each depth were immediately
234 composited and homogenized, and separate subsamples were extracted in solutions of 0.5 M
235 hydrochloric acid (HCl) and 0.2 M sodium citrate/0.05M ascorbic acid within 1 min of sampling.
236 The HCl extraction solubilizes adsorbed and some solid phase Fe(II), and a reactive fraction of
237 Fe(III) minerals (Fredrickson et al. 1998). The low pH of the HCl solution inhibits Fe(II)
238 oxidation prior to analysis. Soil subsamples (3 g dry mass equivalent) were immersed in a 1:10
239 ratio with HCl, vortexed, shaken for 1 h, and filtered to 0.22 μm. We measured concentrations of
240 Fe(II) and Fe(III) colorimetrically using a ferrozine assay (Viollier et al. 2000). We subsequently
241 used Fe(II) concentrations and the ratio of Fe(II) to total Fe in the HCl extraction ($Fe(II)/Fe_{HCl}$)
242 as indices of reducing conditions. Normalizing Fe(II) concentrations by the total Fe_{HCl} pool
243 yields the fraction of the Fe_{HCl} pool that is reduced, thus accounting for differences in Fe_{HCl}
244 among samples. To further assess temporal variation in Fe(II) within and among catena positions,
245 additional soils were collected in February and May 2012 from one of the catenas described

246 above (15 plots x two depth increments) at locations within 0.5 m of the original samples, and
247 were extracted in 0.5 M HCl.

248 We also extracted soils with sodium citrate/ascorbate solution (Reyes and Torrent 1997)
249 to provide an estimate of reducible Fe oxides (Fe_{ca}). This assay reductively dissolves and
250 chelates Fe oxides in proportion to a pool that is potentially reducible by microbes (Hyacinthe et
251 al. 2006). Soil subsamples (1.5 g dry mass equivalent) were combined in a 1:30 ratio with
252 citrate/ascorbate solution in the field, vortexed and then shaken for 18 hr, and centrifuged for 10
253 min at 1500 rcf. We additionally extracted separate soil subsamples with acid ammonium oxalate
254 solution in the dark at pH 3 (Loeppert and Inskeep 1996) to provide a separate index of
255 chelatable Fe and Al (Fe_{ox} and Al_{ox}), omitting removal of carbonates, which are negligible in
256 these soils. Oxalate-extractable metals have been defined as "poorly crystalline" forms in
257 previous studies (Torn et al. 1997; Kleber et al. 2005). This pool may differ subtly from
258 citrate/ascorbate Fe, which reflects Fe solubilized via reductive dissolution and includes a
259 smaller fraction of Fe chelatable by citrate alone. Citrate/ascorbate solution is advantageous as it
260 does not appear to solubilize crystalline minerals (Reyes and Torrent 1997). We used air-dried
261 and ground samples for the oxalate extraction for best comparison with previously published
262 results, and because oxalate can extract crystalline Fe in the presence of Fe(II), which persists in
263 moist soils (Phillips et al. 1993). We note that trends and relative differences in metal
264 concentrations among these extractions are likely to be more meaningful than differences in their
265 absolute magnitude, given that citrate/ascorbate extractions were conducted on field-moist
266 samples whereas oxalate extractions were conducted on air-dried samples according to standard
267 protocols (Loeppert and Inskeep 1996). Our field extractions with citrate/ascorbate are perhaps
268 best representative of the in situ concentrations of short-range order Fe minerals and

associated/substituted Al, as well as Fe and Al in organic complexes. Citrate/ascorbate extractions of field-moist soils (Dubinsky et al. 2010) yielded much higher Fe concentrations than air-dried soils (Reyes and Torrent 1997), presumably due to mineral crystallization. We did not use a sodium pyrophosphate extraction in this study because recent work suggests that much of the Fe solubilized by this method represents nano-crystalline phases rather than organo-Fe complexes (Thompson et al. 2011). We would also expect this nano-crystalline Fe to also contain co-precipitated Al.

Air-dried and ground subsamples were also extracted with sodium citrate/dithionite solution (Loeppert and Inskeep 1996) to measure total free Fe oxides (Fe_{cd}). Dithionite is a stronger reductant than ascorbate and dissolves crystalline Fe minerals such as goethite and hematite. Thus, Fe extracted by citrate/dithionite spans crystalline to poorly-crystalline phases, overlapping the pool extracted by citrate/ascorbate. We estimated the pool of crystalline Fe extractable by citrate/dithionite but not citrate/ascorbate as the difference between these extractions (Fe_{cd-ca}). Iron and Al in soil extractions were analyzed in triplicate via inductively coupled plasma optical emission spectrometry (ICP-OES; Perkin Elmer Optima 5300 DV, Waltham, Massachusetts). Concentrations of Fe_{HCl} determined colorimetrically and via ICP-OES agreed to within 1 %. Soil subsamples for C analysis were air dried and sieved to 2 mm, and visible roots were removed by hand. Samples were ground to a fine powder and analyzed in duplicate for total C by combustion on a CE Elantech elemental analyzer (Lakewood, NJ). Duplicate samples differed by an average of 2 %. Soil C content was corrected for any moisture remaining (0.5 – 2 %) after drying at 105 °C.

The two remaining 6 cm diameter cores from each plot and depth (sample volume = 283 cm^3, total n = 149) were assayed for root biomass and bulk density, respectively. All cores were

sampled quantitatively in 10-cm increments, and no sample compression was evident. Cores for root biomass analysis were sieved with water, and fine roots (≤ 2 mm diameter) were separated into live and dead fractions based on turgor, tensile strength, and integrity of the stele tissue (Silver and Vogt 1993). Roots were thoroughly rinsed in deionized water and dried at 65 °C to constant mass. Bulk density was determined gravimetrically on a separate replicate 6-cm diameter core after correcting for the volume of any rocks (diameter > 2 mm) or coarse roots (diameter > 5 mm), which had a minimal effect (2 %) on bulk density measurements. Soils were dried at 105 □C to constant mass, and bulk density was calculated as dry soil mass divided by the corrected sample volume. We analyzed additional subsamples of field-moist soil from each plot for particle size using the hydrometer method (Gee and Bauder 1986). Organic matter was not removed prior to texture analysis. Samples (50 g dry mass equivalent) were passed through a 2 mm sieve, soaked for 16 h in 50 g l^{-1} sodium hexametaphosphate solution, and dispersed in an electric mixer. We measured changes in soil suspension density over 24 hours to calculate clay, sand, and silt fractions.

2.3 Statistical analysis

We compared site means (n = 6) of soil C and other biogeochemical variables with linear models where variances were allowed to vary among sites using the gls function in R (Pinheiro et al. 2014), with post-hoc comparisons using Tukey's honestly significant difference test. Pairwise relationships among site mean values were assessed using Pearson correlation coefficients. We did not include litterfall NPP in correlation analyses because values were equivalent for different topographic positions in the lower montane forest, resulting in only four independent measurements (lower montane, palo colorado, sierra palm, elfin). We note that

because the montane forest soil analyses were not replicated at different sites within a given forest type, statistical comparisons are restricted to these particular sites, and cannot be generalized to the forest types as a whole.

Relationships between soil C and predictor variables at the scale of individual soil samples (n = 149) were analyzed using linear mixed-effects regression models fit using the lme function in R (Pinheiro et al. 2014). Soil C concentrations and stocks were modeled separately. Models included transects and plots as random effects to account for the spatial structure of our sampling design (samples within plots within sites), thus avoiding pseudoreplication. All of the variables listed in Table 2 were included as potential predictors during model selection. Depth was necessarily included as a blocking factor to account for the structure of the sampling design and any depth-related variation in C not explained by the other predictor variables. We also included interaction terms between Al_{ca} and $Fe(II)/Fe_{HCl}$, and Fe_{ca} and $Fe(II)/Fe_{HCl}$ as potential predictors given the possibility of interactions between reducing conditions and short-range order Fe and Al as discussed in the Introduction. Predictor variables were normalized by mean and standard deviation to allow comparisons of variable importance analogous to Pearson's r. We selected the optimal combination of fixed-effect predictors using stepwise backwards elimination from a model including all potential predictors, using $p < 0.01$ as the significance criterion. We fit separate models for two datasets: the lower montane soils (n = 119), given that they comprised the majority of our samples and experienced a relatively uniform climate, and the lower montane and the montane soils together (n = 149). Two outliers with extremely high Fe(II) concentrations were removed from this analysis. Variance inflation and model matrix condition numbers implied that multicollinearity among variables was unimportant. We present pseudo-R^2

336 values, which correct for the presence of random effects in the models (Nakagawa and
337 Schielzeth 2013).

338 **3. Results**

339 **3.1 Landscape patterns of soil carbon concentrations, stocks, and covariates**

340 Mean C concentrations differed significantly among sites and topographic positions, but
341 were not significantly correlated with long-term mean soil O_2 concentrations at the site scale
342 (Fig. 1a, Supplemental Table 1). Rather, variation in mean site soil C concentrations (0 – 20 cm,
343 n = 6 sites) correlated most strongly with total fine root biomass ($r = 0.99$, $p < 0.001$;
344 Supplemental Table 1) and an index of reducing conditions, Fe(II) ($r = 0.94$, $p < 0.01$). Similarly,
345 the strongest predictors of mean site soil C stocks were total and dead fine root biomass ($r =$
346 0.99, $p < 0.001$ for both variables), and Fe(II) ($r = 0.98$, $p < 0.001$). Concentrations of Fe(II)
347 correlated strongly with both total fine root biomass and dead fine root biomass at the site scale
348 ($r = 0.96$ and 0.94, respectively; $p < 0.01$), and showed a negative correlation with crystalline Fe
349 ($Fe_{cd\text{-}ca}$). Total fine root biomass also correlated positively with Al_{ca} ($r = 0.96$, $p < 0.01$), and
350 negatively with bulk density ($r = -0.97$, $p < 0.01$). Pearson correlations between site mean values
351 of all biogeochemical variables and their statistical significance are reported in Supplemental
352 Table 1.

353 Surface soil (0 – 10 cm) C concentrations were greatest in the palm and elfin forests,
354 intermediate in the palo colorado forest, and lowest in the lower montane forest soils, where C
355 concentrations decreased significantly from ridges to slopes to valleys (Fig. 1a, Supplemental
356 Table 2). Shallow subsurface (10 – 20 cm) C concentrations were significantly greater in the

357 palm, palo colorado, and elfin forests than in the lower montane forest sites, which did not
358 significantly differ from each other (Fig. 1a). In contrast to C concentrations, C stocks in the 0 –
359 10 cm increment were similar among all sites with the exception of the elfin forest. In the 10 –
360 20 cm soils, C content increased as O_2 declined with elevation across the site gradient (ie, from
361 left to right in Fig. 1c). Differing trends in C concentrations and stocks among sites were
362 influenced by variation in bulk density, which differed by a factor of three at the site scale and
363 was greatest in the lower montane valleys and lowest in the palm forest (Fig. 1). Patterns in 0 –
364 10 cm bulk density corresponded strongly with variation in fine root biomass among sites (Fig.
365 1b,d). Bulk density in the 10 – 20 cm depth was less variable and did not differ significantly
366 among sites. Live fine root biomass was greatest in the palm and elfin forests and significantly
367 declined by a factor of two from ridges to valleys in 0 – 10 cm soil (Fig. 1b). Live fine roots
368 exceeded dead fine root biomass in all sites except for the elfin forest, where dead fine root
369 biomass was more than four-fold greater than the other sites (Fig. 1b).

370 Soil Fe pools differed greatly among sites (Fig. 2, Table 3). Concentrations of HCl-
371 extractable Fe(II) increased by more than five-fold between the lower montane and elfin sites,
372 whereas the palm and palo colorado sites had intermediate and highly variable Fe(II)
373 concentrations (Fig. 2a). Trends in the $Fe(II)/Fe_{HCl}$ ratio across sites were similar to those of
374 Fe(II), with fewer significant differences among sites (Supplemental Table 2). In the lower
375 montane forest soils, Fe(II) concentrations were greatest and equivalent in ridge 0 – 10 cm and
376 valley 10 – 20 cm soils over three different sampling events (excluding eight outliers of the 90
377 total samples with Fe(II) > 1000 $\mu g\ g^{-1}$), while concentrations were significantly lower in slope
378 soil at the 10 – 20 cm depth (Supplemental Fig. 1). Crystalline Fe ($Fe_{cd\text{-}ca}$) decreased more than
379 two-fold from lower montane slopes to ridges to valleys, which were similar to the palm and

palo colorado sites; $Fe_{cd\text{-}ca}$ was essentially absent in the elfin site (Fig. 2b). Citrate/ascorbate extractable Fe (Fe_{ca}) concentrations were greatest in the lower montane ridges and lowest in the palo colorado site (Fig. 2b). Oxalate-extractable Fe (Fe_{ox}) concentrations and Fe_{ca} were similar in the palm and elfin forests, but Fe_{ox} was 30 – 60 % lower than Fe_{ca} in the other sites (Fig. 2c). The ratio of Fe_{ca} / Fe_{ox} declined significantly and consistently with decreasing O_2 across all sites (Fig. 2d).

3.2 Pairwise relationships between biogeochemical variables and soil C

We assessed pairwise relationships between all measured biogeochemical variables and C concentrations and stocks at the scale of individual samples (n = 149) as a heuristic evaluation prior to reporting mixed-effects models with multiple explanatory variables later in the text, which included random effects to account for spatial autocorrelation at the scale of plots and sites. We found significant positive linear relationships between C concentrations and Al_{ca}, Al_{ox}, Al_{HCl}, $Fe(II)_{HCl}/Fe_{HCl}$ Fe_{ox}, silt, and fine roots (Fig. 3; R^2 values are reported in the legend). In contrast, we observed negative relationships between C concentrations and $Fe_{cd\text{-}ca}$ and clay. We found similar overall trends between C stocks and predictor variables, although the strength of pairwise relationships frequently differed (Supplemental Fig. 2; R^2 values are reported in the legend). Carbon stocks increased significantly with Al_{ca}, Al_{ox}, Al_{HCl}, $Fe(II)_{HCl}/Fe_{HCl}$ Fe_{ox}, silt, sand, and fine roots. Carbon stocks decreased with $Fe_{cd\text{-}ca}$ and clay. The weak but significant trends between C concentrations and stocks and texture variables (sand, silt, and clay) were driven by extreme values in the montane forest samples (n = 30), as the lower montane samples (n = 119) displayed no significant pairwise relationships with any texture variable when analyzed alone.

3.3 Statistical models for predicting soil C concentrations and stocks

The optimal mixed-effects model for C concentrations in individual soil samples from the lower montane forest (n = 119) showed that C significantly increased with total fine root biomass, Al_{ca}, Fe_{ox}, an index of reducing conditions ($Fe(II)/Fe_{HCl}$), $Fe(III)_{HCl}$, and an interaction between $Fe(II)/Fe_{HCl}$ and Al_{ca}, while C concentrations significantly decreased with depth and Fe_{ca} (Supplemental Table 3). The overall model pseudo R^2 was 0.72, and seven of the eight predictor variables were significant at $p < 0.001$, whereas the remaining variable ($Fe(II)/Fe_{HCl}$ x Al_{ca} interaction) was significant at $p < 0.01$. The optimum model of soil C concentrations for the entire dataset (n = 149) was quite similar to the model for the lower montane samples alone, although it did not include Fe_{HCl}, and the pseudo R^2 value was 0.82.

The optimum model of individual sample soil C stocks for the lower montane soils was broadly consistent with the model of C concentrations, although it contained fewer fixed effects and had much lower explanatory power (pseudo $R^2 = 0.18$; Supplemental Table 4). The model showed that C stocks increased with Fe_{ox} and Al_{ca}, and decreased with Fe_{ca} and depth. The model of C stocks for the overall dataset, in contrast, included more predictor variables and had greater explanatory power (pseudo $R^2 = 0.60$). Overall, C stocks increased with $Fe(II)/Fe_{HCl}$, Fe_{ox}, Al_{ca}, an interaction between $Fe(II)/Fe_{HCl}$ and Al_{ca}, and decreased with Fe_{ca}. This model did not include an effect of soil depth, indicating that the other predictor variables captured the effect of depth on soil C stocks.

4. Discussion

Biogeochemical predictors including reducing conditions, multiple pools of reactive Al and Fe, and fine root biomass could explain a large majority of the spatial variation in surface soil C in sites spanning a broad range of biophysical environments in the Luquillo Experimental Forest. Given the observational nature of this study, we cannot interpret our findings in terms of causation, but we suggest that the patterns observed here reflect underlying biogeochemical mechanisms. Site mean C concentrations and stocks (n = 6) were very strongly related to an index of reducing conditions and root biomass, whereas the mixed-effects models of individual C samples implied the additional importance of several indices of reactive Al and Fe at finer spatial scales. These were indicated by highly significant model coefficients, overall high explanatory power, and a decreased importance of root biomass in the sample-scale mixed-effects model. In contrast, the low R^2 values of univariate pairwise comparisons between C and predictor variables at the scale of individual soil samples indicated the importance of additive and interactive relationships between biogeochemical drivers and soil C concentrations and stocks. It is unsurprising that the mixed-effects models of soil C at the scale of individual samples included additional biogeochemical variables not evident at the coarser scale of sites, as these models had much greater spatial resolution and statistical power to detect relationships between soil C and potential predictors. Additionally, the sample-scale models allowed us to assess the importance of biogeochemical spatial heterogeneity within sites as well as among sites, which was important for teasing apart relationships between soil C and multiple indices of reactive Fe and Al.

Variation in total C among samples was likely driven by changes in both mineral-associated and particulate C. Previous studies have shown a predominance (75 – 90 %, mass basis) of mineral-associated C relative to particulate C across the lower montane tabonuco and palo colorado forests, including the same sites examined here (Cusack et al. 2011; Hall et al.

2015a). Soil C concentrations and stocks often showed distinct patterns among sites due to co-variation in bulk density, as reported by previous studies in the Luquillo Experimental Forest (Johnsen et al. 2015). Variation in bulk density was likely driven predominantly by variation in fine root biomass and consequent impacts on soil aggregation, given the very strong negative correlation between fine roots and bulk density across all sites. In contrast, light fraction C content likely had less impact on variation in bulk density. Light fraction C varied little among topographic positions in the lower montane forest despite high variation in bulk density, and represented a consistently minor portion (13 %) of total soil C (Hall et al., 2015). The sierra palm and elfin forests likely had a greater proportion of particulate C, as suggested by large increases in total soil C concentrations. McGroddy and Silver (2000) found that particulate C comprised approximately 70 % of total soil C in a sparsely forested site at an even higher elevation than the elfin forest examined here, providing a likely upper bound on the contribution of particulate C in the present study. Another recent study in the Luquillo Experimental Forest found that soil C content strongly increased with soil C/N ratios (Johnson et al. 2015). This pattern could reflect the effects of increasing particulate C abundance, given that particulate C has a greater C/N ratio than mineral-associated C (Cusack et al. 2011). Despite likely differences in the proportion of mineral-associated vs. particulate C among sites, it is notable that predictors of total soil C in mixed-effects models were highly similar when comparing the lower montane sites alone (which had very little particulate C) with the entire dataset.

We have no data describing soil organic matter turnover rates in the montane sites examined here, but mineral-associated C turnover was well constrained in the lower montane forest using radiocarbon measurements and modeling in a separate study. The majority (66 %) of mineral-associated C sampled across a topographic catena turned over rapidly (11 – 26 y) (Hall

et al., 2015). In that study, increasing Fe(II) concentrations were associated with longer turnover times of mineral-associated C, and were the only variable significantly related to turnover rates. In the lower montane forest, we expect that variation in C concentrations was primarily driven by mineral-associated C abundance, given that the relatively small pool of particulate C in these sites (13 ± 2 % of total C; Hall et al., 2015) would not be large enough to explain the high variability in total C concentrations among samples. However, in the montane forest it is likely that strongly reducing conditions and high root biomass allocation contributed to particulate C accumulation, possibly analogous to a mineral-rich peatland soil (Fenner and Freeman 2011).

4.1 Relationships between litterfall, fine root biomass, and soil C content

Spatial patterns in soil C among sites appeared to primarily reflect variation in factors controlling soil organic matter decomposition rates as opposed to C inputs. Soil C concentrations and stocks increased with site-level indices of reducing conditions even as litterfall, a proxy for NPP, decreased. A similar pattern of decreasing aboveground C inputs and increasing soil C was observed across an elevation gradient of Hawaiian tropical montane forests (Schuur et al. 2001). However, relationships between soil C and root biomass were more difficult to interpret. Given that litterfall declined at the site scale as root biomass increased, the strong and highly significant pairwise relationships observed between fine root biomass and soil C at the site scale were unlikely to reflect increased C inputs from higher root productivity. Rather, the accumulation of high root standing stocks (dominated by dead biomass at the montane sites) may simply reflect low rates of particulate organic matter decomposition under reducing conditions, leading to an increased particulate fraction of soil C. Increased root biomass could also reflect plant nutrient limitation and long-term investment in root biomass to promote nutrient acquisition, but not

necessarily reflect increased root productivity (Vogt et al. 1996; Ostertag 2001; Espeleta and Clark 2007). Regardless of the degree to which fine root biomass stocks may reflect C inputs vs. rates of C losses, fine root biomass provided an exceptionally strong proxy for surface soil C concentrations at the site scale, but was much less important in mixed-effects models of soil C at the scale of individual samples after other covariates were accounted for.

4.2 Reducing conditions and C accumulation

We observed very strong relationships between an index of reducing conditions (Fe(II) concentrations) and soil C at the scale of sites and individual samples, indicative of the overall importance of anaerobiosis in retarding decomposition. Recent studies have also showed the importance of periodic anaerobiosis in promoting C mobilization and degradation (Thompson et al. 2006; Hall and Silver 2013; Hall et al. 2014; Buettner et al. 2014; Hall et al. 2015b), although our present data suggest that inhibitory effects of anaerobiosis on organic matter decomposition may predominate at the landscape scale. The Fe(II) concentrations that we measured, especially in the montane palm, palo colorado, and elfin forest sites, were similar to those measured in flooded wetland sediments and rice paddy soils under anaerobic conditions (Roden and Wetzel 1996; Frenzel et al. 1999). In the upland, non-flooded soils examined here, high Fe(II) concentrations and differences between soil O_2 and Fe(II) among sites likely reflect the prevalence of reducing conditions in microsites within a porous soil matrix, which typically contains substantial gas-phase O_2 (Silver et al. 1999).

4.3 Multiple relationships between Fe pools and soil C

510 Crystalline Fe oxides (Fe_{cd-ca}) declined precipitously with mean soil O_2 across sites at the
511 landscape scale, presumably reflecting weathering over pedogenic timescales, whereas Fe_{ox}
512 varied relatively little. Thompson et al. (2011) observed a similar pattern across a Hawaiian
513 gradient of basaltic soils, where increased precipitation depleted Fe oxyhydroxides while organic
514 and silicate-bound Fe were retained. The ratio of Fe_{ca} to Fe_{ox} also showed a consistent decline
515 with mean soil O_2 across sites. We hypothesize that this pattern might reflect the progressive
516 depletion of excess Fe_{ca} relative to Fe_{ox} by reductive dissolution and leaching, along with the
517 relative retention of Fe co-precipitated with organic matter and/or Al, which could be less
518 vulnerable to reductive dissolution. Supporting this idea, Varela and Tien (2003) demonstrated
519 that high concentrations of organic ligands can inhibit Fe reduction. Whereas Fe_{ox} represented a
520 dominant Fe fraction in the sites with greatest soil C concentrations and lowest O_2, crystalline Fe
521 (Fe_{cd-ca}) was negligible. The lack of a relationship between crystalline Fe and C is unsurprising
522 given that it has relatively less reactive surface area than short range-order Fe phases likely
523 represented by Fe_{ox}.

524 Co-variation in Fe_{ca}/Fe_{ox} and C at the site scale may help explain opposing relationships
525 between soil C concentrations and these two Fe pools in the mixed-effects models of individual
526 soil samples. Mixed-effects models allowed us to test relationships between soil C and multiple
527 co-varying predictor variables while including random effects to account for spatial correlation.
528 Positive relationships between Fe_{ox} and soil C are consistent with a wide body of work reflecting
529 the importance of Fe-C sorption and co-precipitation in protecting C from microbial
530 decomposition (e.g. Kaiser and Guggenberger 2000; Powers and Schlesinger 2002; Kleber et al.
531 2005). More interesting, however, was the highly significant negative relationship between C
532 concentrations and Fe_{ca}, which was consistent regardless of whether Fe_{ox} was included in the

533 mixed-effects models or not. We hypothesize that this relationship reflects the importance of Fe
534 reduction as a mechanism of C loss. In other words, the availability of excess reducible, short-
535 range order Fe oxides to catalyze anaerobic microbial respiration in humid tropical ecosystems
536 may partially offset soil C accumulation under reducing conditions, despite the fact that organo-
537 Fe interactions are also demonstrably associated with C accumulation. Dissimilatory Fe
538 reduction is the dominant anaerobic respiratory process in these soils and accounts for a
539 significant portion of ecosystem metabolism (Dubinsky et al. 2010), and anaerobic
540 decomposition has been shown to increase with the availability of reactive Fe oxides (Sutton-
541 Grier et al. 2011). Short-term respiration rates are similar under aerobic and anaerobic conditions
542 in soils from lower montane forest ridges (McNicol and Silver 2014), exemplifying the
543 importance of Fe reduction in sustaining high rates of decomposition. These multiple
544 biogeochemical functions of reactive Fe could help explain multiple relationships—positive,
545 negative, and neutral—previously reported between Fe measured in different soil extractions and
546 C concentrations in humid tropical ecosystems (Powers and Schlesinger 2002; Koning et al.
547 2003; Powers and Veldkamp 2005; Tonneijck et al. 2010). Further work is needed to assess the
548 multiple potential roles of Fe in soil C cycling, especially the characterization of pools isolated
549 by extractions and their spatial relationship with organic matter.

550 **4.4 Relationships between extractable Al and soil C**

551 Concentrations of Al_{ca} were the strongest individual correlate of sample-scale C
552 concentrations in mixed-effects models. While the precise speciation of Al_{ca} is uncertain, it likely
553 includes a substantial portion of organically-complexed Al as well as Al co-precipitated with
554 short-range order Fe oxides. The positive relationship between Al_{ca} and C concentrations and

555 stocks suggests the importance of organo-Al complexation, cation bridging, and possibly C
556 sorption to short-range ordered Al minerals in contributing to C stabilization in soils across the
557 landscape. Similar patterns are apparent across a wide range of soil types, although they have
558 predominantly been demonstrated in Andisols (Torn et al. 1997; Percival et al. 2000; Powers and
559 Schlesinger 2002; Kleber et al. 2005; Wagai and Mayer 2007; Tonneijck et al. 2010).
560 Meanwhile, clay content showed no relationship with soil C concentrations or stocks, similar to
561 the findings of Percival et al. (2000). The absence of a relationship between soil C and clay
562 content is unsurprising in these soils given that they are dominated by kaolinite (Peretyazhko and
563 Sposito 2005), which is less reactive than the 2:1 phyllosilicate clays.

564 One implication of the mixed-effects models is that reducing conditions and the co-
565 precipitation or sorption of organic compounds by reactive Al appear to have additive impacts on
566 organic matter accumulation, or possibly promote the accumulation of different forms of C
567 (particulate vs. mineral-associated). In addition, the mixed-effects models suggested a strong
568 interactive relationship between Al_{ca} and reducing conditions, where simultaneous increases in
569 concentrations of Al_{ca} and Fe(II) were associated with greater C than expected from either
570 variable alone. This relationship may simply indicate the importance of some other unmeasured
571 covariate that led to C accumulation in samples that were especially rich in Al_{ca} and Fe(II), or it
572 could be indicative of an underlying mechanism. For example, the positive interaction between
573 Al_{ca} and reducing conditions with soil C concentrations might also imply the importance of
574 molecular O_2 as a co-reactant to decompose organic matter associated with Al, given that
575 oxidase enzymes and reactive oxygen species are well known to be potent agents of organic
576 matter solubilization (Sinsabaugh 2010) that could disrupt metal/organic complexes.

5. Conclusions

In current conceptual frameworks of soil C cycling in upland ecosystems, sorption and complexation of organic matter by reactive metals and minerals are thought to strongly influence spatial patterns of soil C accumulation, whereas the availability and influence of O_2 and other oxidants (e.g. Fe oxides) on decomposition have received less attention. Previous studies of soil C in humid tropical forests often focused on relationships between C and soil mineralogy and geochemistry. We found that a relatively small suite of variables, including a proxy for reducing conditions, multiple indices of reactive Fe and Al, and fine root biomass could explain a majority of the variation in C concentrations and stocks across a humid tropical forest landscape. Co-variation among fine root biomass, reducing conditions, and soil C likely reflected impacts of reducing conditions on organic matter decomposition rates. Mixed-effects models also suggested the importance of a positive interaction between reducing conditions and Al-organic complexation in promoting C accumulation. We found, however, that C concentrations declined with the availability of reducible Fe (citrate/ascorbate extraction) that can sustain anaerobic microbial respiration, independent of the positive relationships between C and reducing conditions and Fe_{ox}. Our findings imply the importance of nuanced and multifaceted relationships between reducing conditions, roots, and reactive metals/minerals in understanding the distribution of soil organic matter in humid tropical forests, which represent exceptionally productive ecosystems with important links to the global climate system.

Acknowledgements

All data reported here will be publicly available through the NSF Critical Zone Observatory web data repository (http://criticalzone.org/luquillo/data/). We thank T. Baisden, M.

Kramer, and anonymous reviewers for critical commentary. G. Sposito, A. Thompson, M. Firestone, and R. Rhew also provided valuable insights, and H. Dang, J. Treffkorn, T. Natake, J. Cosgrove, R. Ryals, A. McDowell, and C. Torrens helped in the field and lab. SJH was funded by the DOE Office of Science Graduate Fellowship Program supported by the American Recovery and Reinvestment Act of 2009, administered by ORISE-ORAU under contract no. DE-AC05-06OR23100. WLS received support from CA-B-ECO-7673-MS from the A.E.S. Funding was also provided by DOE grant DE-FOA-0000749 and NSF grant EAR-08199072 to WLS, the NSF Luquillo Critical Zone Observatory (EAR-0722476) with additional support provided by the USGS Luquillo WEBB program, and grant DEB 0620910 from NSF to the Institute for Tropical Ecosystem Studies, University of Puerto Rico, and to the International Institute of Tropical Forestry USDA Forest Service, as part of the LTER Program.

References

Baldock JA, Skjemstad JO (2000) Role of the soil matrix and minerals in protecting natural organic materials against biological attack. Org Geochem 31:697–710. doi: 10.1016/S0146-6380(00)00049-8

Bruun TB, Elberling B, Christensen BT (2010) Lability of soil organic carbon in tropical soils with different clay minerals. Soil Biol Biochem 42:888–895. doi: 10.1016/j.soilbio.2010.01.009

Buettner SW, Kramer MG, Chadwick OA, Thompson A (2014) Mobilization of colloidal carbon during iron reduction in basaltic soils. Geoderma 221–222:139–145. doi: 10.1016/j.geoderma.2014.01.012

Christensen TH, Bjerg PL, Banwart SA, et al (2000) Characterization of redox conditions in groundwater contaminant plumes. J Contam Hydrol 45:165–241. doi: 10.1016/S0169-7722(00)00109-1

Cleveland CC, Wieder WR, Reed SC, Townsend AR (2010) Experimental drought in a tropical rain forest increases soil carbon dioxide losses to the atmosphere. Ecology 91:2313–2323. doi: 10.1890/09-1582.1

626 Cusack DF, Chou WW, Yang WH, et al (2009) Controls on long-term root and leaf litter
627 decomposition in neotropical forests. Global Change Biol 15:1339–1355. doi:
628 10.1111/j.1365-2486.2008.01781.x

629 Cusack DF, Silver WL, Torn MS, McDowell WH (2011) Effects of nitrogen additions on above-
630 and belowground carbon dynamics in two tropical forests. Biogeochemistry 104:203–225.
631 doi: 10.1007/s10533-010-9496-4

632 DeAngelis KM, Chivian D, Fortney JL, et al (2013) Changes in microbial dynamics during long-
633 term decomposition in tropical forests. Soil Biology and Biochemistry 66:60–68. doi:
634 10.1016/j.soilbio.2013.06.010

635 Dieleman WIJ, Venter M, Ramachandra A, et al (2013) Soil carbon stocks vary predictably with
636 altitude in tropical forests: Implications for soil carbon storage. Geoderma 204–205:59–
637 67. doi: 10.1016/j.geoderma.2013.04.005

638 Dubinsky EA, Silver WL, Firestone MK (2010) Tropical forest soil microbial communities
639 couple iron and carbon biogeochemistry. Ecology 91:2604–2612. doi: 10.1890/09-1365.1

640 Espeleta JF, Clark DA (2007) Multi-scale variation in fine-root biomass in a tropical rain forest:
641 a seven-year study. Ecol Monogr 77:377–404. doi: 10.1890/06-1257.1

642 Fredrickson JK, Zachara JM, Kennedy DW, et al (1998) Biogenic iron mineralization
643 accompanying the dissimilatory reduction of hydrous ferric oxide by a groundwater
644 bacterium. Geochim Cosmochim Ac 62:3239–3257. doi: 10.1016/S0016-7037(98)00243-
645 9

646 Frenzel P, Bosse U, Janssen PH (1999) Rice roots and methanogenesis in a paddy soil: ferric iron
647 as an alternative electron acceptor in the rooted soil. Soil Biol Biochem 31:421–430. doi:
648 10.1016/S0038-0717(98)00144-8

649 Gee G, Bauder J (1986) Particle size analysis. In: Klute A (ed) Methods of Soil Analysis, Part 1,
650 Physical and Mineralogical Methods, 2nd edn. American Society of Agronomy, Madison,
651 WI, USA, pp 383–411

652 Hall SJ, McDowell WH, Silver WL (2013) When wet gets wetter: Decoupling of moisture, redox
653 biogeochemistry, and greenhouse gas fluxes in a humid tropical forest soil. Ecosystems
654 16:576–589. doi: 10.1007/s10021-012-9631-2

655 Hall SJ, McNicol G, Natake T, Silver WL (2015a) Large fluxes and rapid turnover of mineral-
656 associated carbon across topographic gradients in a humid tropical forest: insights from
657 paired 14C analysis. Biogeosciences Discuss 12:891–932. doi: 10.5194/bgd-12-891-2015

658 Hall SJ, Silver WL (2013) Iron oxidation stimulates organic matter decomposition in humid
659 tropical forest soils. Glob Chang Biol 19:2804–2813. doi: 10.1111/gcb.12229

660 Hall SJ, Silver WL, Timokhin VI, Hammel KE (2015b) Lignin decomposition is sustained under
661 fluctuating redox conditions in humid tropical forest soils. Glob Chang Biol 21:2818-
662 2828. doi: 10.1111/gcb.12908

663 Hall SJ, Treffkorn J, Silver WL (2014) Breaking the enzymatic latch: Impacts of reducing
664 conditions on hydrolytic enzyme activity in tropical forest soils. Ecology 95:2964–2973.
665 doi: 10.1890/13-2151.1

666 Heartsill Scalley T, Scatena FN, Lugo AE, et al (2010) Changes in structure, composition, and
667 nutrients during 15 yr of hurricane-induced succession in a subtropical wet forest in
668 Puerto Rico. Biotropica 42:455–463. doi: 10.1111/j.1744-7429.2009.00609.x

669 Hyacinthe C, Bonneville S, Van Cappellen P (2006) Reactive iron(III) in sediments: Chemical
670 versus microbial extractions. Geochim Cosmochim Ac 70:4166–4180. doi:
671 10.1016/j.gca.2006.05.018

672 Jobbagy EG, Jackson RB (2000) The vertical distribution of soil organic carbon and its relation
673 to climate and vegetation. Ecol Appl 10:423–436. doi: 10.1890/1051-
674 0761(2000)010[0423:TVDOSO]2.0.CO;2

675 Johnson AH, Xing HX, Scatena FN (2015) Controls on soil carbon stocks in El Yunque National
676 Forest, Puerto Rico. Soil Science Society of America Journal 79:294. doi:
677 10.2136/sssaj2014.05.0199

678 Kaiser K, Guggenberger G (2000) The role of DOM sorption to mineral surfaces in the
679 preservation of organic matter in soils. Org Geochem 31:711–725. doi: 10.1016/S0146-
680 6380(00)00046-2

681 Kleber M, Mikutta R, Torn MS, Jahn R (2005) Poorly crystalline mineral phases protect organic
682 matter in acid subsoil horizons. Eur J Soil Sci 56:717–725. doi: 10.1111/j.1365-
683 2389.2005.00706.x

684 Koning GHJ de, Veldkamp E, López-Ulloa M (2003) Quantification of carbon sequestration in
685 soils following pasture to forest conversion in northwestern Ecuador. Global Biogeochem
686 Cycles 17:1098. doi: 200310.1029/2003GB002099

687 Kramer MG, Sanderman J, Chadwick OA, et al (2012) Long-term carbon storage through
688 retention of dissolved aromatic acids by reactive particles in soil. Global Change Biology
689 18:2594–2605. doi: 10.1111/j.1365-2486.2012.02681.x

690 Liptzin D, Silver WL, Detto M (2011) Temporal dynamics in soil oxygen and greenhouse gases
691 in two humid tropical forests. Ecosystems 14:171–182. doi: 10.1007/s10021-010-9402-x

692 Loeppert R, Inskeep W (1996) Iron. In: Sparks D (ed) Methods of Soil Analysis, Part 3--
693 Chemical Methods. Soil Science Society of America, Madison, WI, USA, pp 639–664

694 Malhi Y, Grace J (2000) Tropical forests and atmospheric carbon dioxide. Trends Ecol Evol
695 15:332–337. doi: 10.1016/S0169-5347(00)01906-6

McDowell WH, Scatena FN, Waide RB, et al (2012) Geographic and ecological setting of the Luquillo Mountains. In: Brokaw N, Crowl T, Lugo A, et al (eds) A Caribbean Forest Tapestry: The Multidimensional Nature of Disturbance and Response. Oxford University Press, New York, USA, pp 72–163

McGroddy M, Silver WL (2000) Variations in belowground carbon storage and soil CO2 flux rates along a wet tropical climate gradient. Biotropica 32:614–624.

McNicol G, Silver WL (2014) Separate effects of flooding and anaerobiosis on soil greenhouse gas emissions and redox sensitive biogeochemistry. J Geophys Res Biogeosci 2013JG002433. doi: 10.1002/2013JG002433

Nakagawa S, Schielzeth H (2013) A general and simple method for obtaining R2 from generalized linear mixed-effects models. Method Ecol Evo 4:133–142. doi: 10.1111/j.2041-210x.2012.00261.x

Ostertag R (2001) Effects of nitrogen and phosphorus availability on fine-root dynamics in Hawaiian montane forests. Ecology 82:485–499. doi: 10.1890/0012-9658(2001)082[0485:EONAPA]2.0.CO;2

Parton W, Silver WL, Burke IC, et al (2007) Global-scale similarities in nitrogen release patterns during long-term decomposition. Science 315:361–364. doi: 10.1126/science.1134853

Percival HJ, Parfitt RL, Scott NA (2000) Factors controlling soil carbon levels in New Zealand grasslands. Soil Science Society of America Journal 64:1623. doi: 10.2136/sssaj2000.6451623x

Peretyazhko T, Sposito G (2005) Iron(III) reduction and phosphorous solubilization in humid tropical forest soils. Geochim Cosmochim Ac 69:3643–3652. doi: 10.1016/j.gca.2005.03.045

Phillips EJP, Lovley DR, Roden EE (1993) Composition of non-microbially reducible Fe(III) in aquatic sediments. Appl Environ Microbiol 59:2727–2729.

Pinheiro J, Bates D, DebRoy S, et al (2014) nlme: Linear and Nonlinear Mixed Effects Models.

Ponnamperuma FN (1972) The chemistry of submerged soils. Adv Agron 24:29–96.

Powers JS, Schlesinger WH (2002) Relationships among soil carbon distributions and biophysical factors at nested spatial scales in rain forests of northeastern Costa Rica. Geoderma 109:165–190. doi: 10.1016/S0016-7061(02)00147-7

Powers JS, Veldkamp E (2005) Regional variation in soil carbon and δ13C in forests and pastures of northeastern Costa Rica. Biogeochemistry 72:315–336. doi: 10.1007/s10533-004-0368-7

Rasse DP, Rumpel C, Dignac M-F (2005) Is soil carbon mostly root carbon? Mechanisms for a specific stabilisation. Plant Soil 269:341–356. doi: 10.1007/s11104-004-0907-y

731 Reyes I, Torrent J (1997) Citrate-ascorbate as a highly selective extractant for poorly crystalline
732 iron oxides. Soil Sci Soc Am J 61:1647–1654.

733 Roden E, Wetzel R (1996) Organic carbon oxidation and suppression of methane production by
734 microbial Fe(III) oxide reduction in vegetated and unvegetated freshwater wetland
735 sediments. Limnol Oceanogr 41:1733–1748.

736 Schuur EAG (2001) The effect of water on decomposition dynamics in mesic to wet Hawaiian
737 montane forests. Ecosystems 4:259–273. doi: 10.1007/s10021-001-0008-1

738 Schuur EAG, Chadwick OA, Matson PA (2001) Carbon cycling and soil carbon storage in mesic
739 to wet Hawaiian montane forests. Ecology 82:3182–3196. doi: 10.1890/0012-
740 9658(2001)082[3182:CCASCS]2.0.CO;2

741 Silver WL, Liptzin D, Almaraz M (2013) Soil redox dynamics and biogeochemistry along a
742 tropical elevation gradient. In: Gonzalez G, Willig MR, Waide RB (eds) Ecological
743 Gradient Analyses in a Tropical Landscape. Wiley, NJ, USA,

744 Silver WL, Lugo AE, Keller M (1999) Soil oxygen availability and biogeochemistry along
745 rainfall and topographic gradients in upland wet tropical forest soils. Biogeochemistry
746 44:301–328. doi: 10.1023/A:1006034126698

747 Silver WL, Vogt KA (1993) Fine-root dynamics following single and multiple disturbances in a
748 subtropical wet forest ecosystem. J Ecol 81:729–738.

749 Sinsabaugh RL (2010) Phenol oxidase, peroxidase and organic matter dynamics of soil. Soil Biol
750 Biochem 42:391–404.

751 Sutton-Grier AE, Keller JK, Koch R, et al (2011) Electron donors and acceptors influence
752 anaerobic soil organic matter mineralization in tidal marshes. Soil Biol Biochem
753 43:1576–1583. doi: 10.1016/j.soilbio.2011.04.008

754 Teh YA, Silver WL, Scatena FN (2009) A decade of belowground reorganization following
755 multiple disturbances in a subtropical wet forest. Plant Soil 323:197–212. doi:
756 10.1007/s11104-009-9926-z

757 Thompson A, Chadwick OA, Boman S, Chorover J (2006) Colloid mobilization during soil iron
758 redox oscillations. Environ Sci Technol 40:5743–5749. doi: 10.1021/es061203b

759 Thompson A, Rancourt D, Chadwick O, Chorover J (2011) Iron solid-phase differentiation along
760 a redox gradient in basaltic soils. Geochim Cosmochim Ac 75:119–133. doi:
761 10.1016/j.gca.2010.10.005

762 Tonneijck FH, Jansen B, Nierop KGJ, et al (2010) Towards understanding of carbon stocks and
763 stabilization in volcanic ash soils in natural Andean ecosystems of northern Ecuador. Eur
764 J Soil Sci 61:392–405. doi: 10.1111/j.1365-2389.2010.01241.x

765 Torn MS, Trumbore SE, Chadwick OA, et al (1997) Mineral control of soil organic carbon
766 storage and turnover. Nature 389:170–173. doi: 10.1038/38260

767 Varela E, Tien M (2003) Effect of pH and oxalate on hydroquinone-derived hydroxyl radical
768 formation during brown rot wood degradation. Appl Environ Microbiol 69:6025–6031.
769 doi: 10.1128/AEM.69.10.6025-6031.2003

770 Viollier E, Inglett P, Hunter K, et al (2000) The ferrozine method revisited: Fe(II)/Fe(III)
771 determination in natural waters. Appl Geochem 15:785–790. doi: 10.1016/S0883-
772 2927(99)00097-9

773 Vogt KA, Vogt DJ, Palmiotto PA, et al (1996) Review of root dynamics in forest ecosystems
774 grouped by climate, climatic forest type and species. Plant Soil 187:159–219. doi:
775 10.1007/BF00017088

776 Wagai E, Mayer L (2007) Sorptive stabilization of organic matter in soils by hydrous iron oxides.
777 Geochim Cosmochim Ac 71:25–35. doi: 10.1016/j.gca.2006.08.047

778 Wagai R, Mayer LM, Kitayama K, Shirato Y (2011) Association of organic matter with iron and
779 aluminum across a range of soils determined via selective dissolution techniques coupled
780 with dissolved nitrogen analysis. Biogeochemistry 112:95–109. doi: 10.1007/s10533-
781 011-9652-5

782 Weaver PL, Medina E, Pool D, et al (1986) Ecological Observations in the Dwarf Cloud Forest
783 of the Luquillo Mountains in Puerto Rico. Biotropica 18:79–85. doi: 10.2307/2388367

784 **Tables**

785 Table 1: Site characteristics. Above-ground litterfall represents annual means (SE) from 1994 –
786 2002 from the palm, palo colorado, and elfin sites, based on monthly litter collection from five
787 replicate baskets per site (W. Silver, unpublished data). Bisley (lower montane forest) data
788 represent bi-weekly litter collections from 60 baskets for 18 months in 1988-89, spanning ridge,
789 slope, and valley positions (Scatena et al., 1996). Bisley litterfall NPP was similar among
790 topographic positions (US Forest Service International Institute for Tropical Forestry,
791 unpublished data).

Site	Elevation (m)	N (°)	W (°)	Total aboveground litterfall (g m^{-2} yr^{-1})

Bisley ridges (n = 4)	240 - 300	18.3157	65.7487	
Bisley slopes (n = 4)	220 - 280	--	--	870 (70)
		--	--	
Bisley valleys (n = 4)	210 - 240	--	--	
Palm	614	18.2988	65.7803	470 (107)
Palo colorado	736	18.2942	65.7852	560 (90)
Elfin	936	18.2702	65.761	366 (55)

792

793 Table 2: Potential predictors of soil C concentrations and stocks in mixed-effects models.
794 Citrate/ascorbate and HCl extractions were conducted on moist soils in the field, and the other
795 extractions were conducted on air-dried soils. See Section 2.2 for details of soil analyses.

Variable	Description	Interpretation
Fe_{ca}	Citrate/ascorbate-extractable Fe	Reducible short-range order (oxy)hydroxides and organo-Fe complexes
Al_{ca}	Citrate/ascorbate-extractable Al	Al substituted in reducible short-range order Fe (oxy)hydroxides and organo-Al complexes
Fe_{ox}	Ammonium oxalate-extractable Fe	Chelatable short-range order (oxy)hydroxides and organo-Fe complexes
Al_{ox}	Ammonium oxalate-extractable Al	Chelatable short-range order (oxy)hydroxides and organo-Al complexes

$Fe(III)_{HCl}$	Fe(III) in 0.5 M HCl	Weak acid soluble short-range order and organo-Fe complexes
Al_{HCl}	Al in 0.5 M HCl	Weak acid soluble short-range order and organo-Al complexes
$Fe(II)/Fe_{HCl}$	Ratio of Fe(II) to total Fe in 0.5 M HCl	Weak acid soluble Fe(II) normalized by Fe_{HCl}
Fe_{cd}	Fe in citrate/dithionite extractions	Total free Fe oxides (crystalline and short-range order)
Fe_{cd-ca}	Fe in citrate/dithionite extractions minus Fe_{ca}	Crystalline Fe oxides (e.g. goethite and hematite)
Fine roots	Roots ≤ 2 mm	Live + dead fine roots
Depth	0 – 10 and 10 – 20 cm increments	
Clay	Particles < 2 μm	
Sand	Particles 50 - 2000 μm	
Silt	Particles 2 - 50 μm	

796

797

Table 3: Soil attributes by site and depth increment. Values represent means and standard errors; n = 20 for each depth increment in the ridge, slope, and valley sites, and n = 5 for the palm, palo colorado, and cloud sites. See Table 2 for abbreviations and Section 2.2 for details of soil analyses. Citrate/ascorbate and HCl extractions were conducted on moist soils in the field, and the other extractions were conducted on air-dried and ground soils.

Site	Depth (cm)	Bulk density ($g\ cm^{-3}$)	Soil C ($mg\ g^{-1}$)	Soil C ($mg\ cm^{-3}$)	Live fine roots ($mg\ cm^{-3}$)	Total fine roots ($mg\ cm^{-3}$)	Sand (%)	Silt (%)	Clay (%)
Ridge	0 - 10	0.47 (0.02)	59 (3)	27 (2)	2.3 (0.2)	3 (0.3)	8 (1)	53 (2)	39 (2)
	10 – 20	0.7 (0.04)	37 (2)	25 (2)	1 (0.2)	1.4 (0.2)	7 (0)	48 (2)	45 (2)
Slope	0 - 10	0.54 (0.04)	51 (4)	26 (2)	1.7 (0.3)	2.3 (0.3)	10 (1)	53 (2)	38 (2)
	10 – 20	0.79 (0.03)	28 (2)	22 (1)	0.9 (0.3)	1.2 (0.3)	12 (1)	49 (2)	39 (2)
Valley	0 - 10	0.65 (0.02)	42 (2)	27 (1)	1 (0.2)	1.5 (0.2)	23 (2)	51 (2)	26 (1)
	10 – 20	0.7 (0.03)	34 (2)	23 (1)	0.6 (0.1)	0.9 (0.2)	23 (2)	47 (2)	30 (2)
Palm	0 - 10	0.24 (0.05)	124 (23)	27 (5)	3.9 (0.7)	4.5 (0.6)	10 (3)	49 (1)	41 (3)
	10 – 20	0.68 (0.06)	49 (5)	33 (2)	2 (0.4)	2.5 (0.4)	12 (1)	53 (2)	35 (1)
Palo colorado	0 - 10	0.51 (0.04)	71 (11)	36 (5)	1.9 (0.5)	3.2 (0.6)	56 (5)	25 (3)	19 (3)
	10 – 20	0.6 (0.08)	70 (11)	40 (6)	2.4 (0.8)	3.9 (1.2)	56 (3)	23 (2)	21 (2)
Elfin	0 - 10	0.35 (0.01)	175 (21)	60 (5)	5.5 (1)	11.4 (1.4)	22 (1)	64 (1)	15 (1)
	10 – 20	0.6 (0.03)	146 (20)	86 (10)	1.1 (0.4)	8.2 (1.2)	22 (1)	62 (1)	16 (1)

Site	Depth (cm)	$Fe(III)_{HCl}$ ($mg\ g^{-1}$)	$Fe(II)_{HCl}$ ($mg\ g^{-1}$)	Fe_{cd} ($mg\ g^{-1}$)	Fe_{cd-ca} ($mg\ g^{-1}$)	Fe_{ca} ($mg\ g^{-1}$)	Fe_{ox} ($mg\ g^{-1}$)	Al_{HCl} ($mg\ g^{-1}$)	Al_{ca} ($mg\ g^{-1}$)	Al_{ox} ($mg\ g^{-1}$)
Ridge	0 - 10	3.5 (0.3)	0.46 (0.04)	44 (1.7)	20.4 (2)	23.6 (1)	9.4 (0.5)	1.7 (0.1)	5 (0.3)	2.3 (0.1)
	10 – 20	3.2 (0.2)	0.25 (0.02)	49.8 (2.1)	27.6 (2.9)	22.2 (1.5)	8.7 (0.4)	1.7 (0.2)	4.1 (0.4)	2.3 (0.1)
Slope	0 - 10	2.4 (0.2)	0.27 (0.04)	45 (2)	28.9 (2)	16.2 (0.8)	7.8 (0.6)	2.1 (0.5)	4 (0.4)	3.1 (0.5)
	10 – 20	1.8 (0.2)	0.11 (0.02)	49 (2.2)	34.2 (2.7)	14.8 (1)	6.6 (0.7)	1.6 (0.2)	2.9 (0.2)	2.7 (0.3)
Valley	0 - 10	2.4 (0.2)	0.38 (0.11)	27.1 (1.5)	10.1 (1.3)	17 (0.7)	9.9 (0.5)	1.3 (0.1)	1.9 (0.1)	2 (0.1)

	10 – 20	2.4 (0.3)	0.43 (0.19)	30.2 (1.7)	14.1 (1.7)	16 (0.9)	10 (0.5)	1.3 (0.1)	1.7 (0.1)	2.1 (0.1)
Palm	0 - 10	3.9 (0.6)	1.22 (0.44)	31.2 (3.6)	12.9 (3.2)	18.3 (1.9)	12.5 (0.7)	3.3 (0.7)	6.6 (1)	4.3 (0.7)
	10 – 20	3.2 (0.3)	0.7 (0.2)	34.3 (3.6)	15.5 (2.9)	18.9 (1.4)	12.8 (0.8)	3.3 (0.7)	7 (1.5)	4.8 (1)
Palo colorado	0 - 10	2.8 (0.6)	1.35 (0.8)	14.2 (3.9)	6.8 (2.5)	7.3 (1.6)	6.5 (1.4)	1.8 (0.2)	4 (0.5)	2.3 (0.3)
	10 – 20	3.5 (1.1)	2.69 (1.21)	15.6 (4.2)	8.3 (2.9)	7.3 (1.5)	6.8 (1.4)	1.8 (0.2)	4.3 (0.4)	2.5 (0.2)
Elfin	0 - 10	4.7 (0.7)	3.74 (0.77)	11 (0.8)	1.1 (0.6)	13.9 (3.7)	14.3 (1.4)	4 (0.6)	6.7 (0.7)	4.8 (0.3)
	10 – 20	5.4 (1)	4.11 (0.79)	11 (2.4)	0.3 (0.3)	12.5 (2)	13.3 (2.3)	4.1 (0.4)	5.8 (0.5)	5 (0.3)

802 **Figure Captions**

803 Figure 1: Means (SE) of soil attributes by depth increment across the site gradient; mean bulk
804 soil O_2 concentrations decreased by site from left to right. For the ridge, slope, and valley sites, n
805 = 20 for each bar, and for the palm, palo colorado, and elfin sites, n = 5 per bar.

806

807 Figure 2: Means (SE) of soil attributes by depth increment across the site gradient; mean bulk
808 soil O_2 concentrations decreased by site from left to right. (a) Concentrations of Fe(II) and
809 Fe(III) in 0.5 M HCl extractions. (b) Fe citrate/ascorbate extractions (Fe_{ca}) and citrate/dithionite
810 extractions (Fe_{cd}), where the total bar height represents Fe_{cd}. The hashed portion represents
811 excess Fe in dithionite extractions relative to citrate/ascorbate (Fe_{cd-ca}; the difference between
812 citrate/dithionite and citrate/ascorbate extractions), which we interpreted as crystalline Fe. (c) Fe
813 in ammonium oxalate extractions (Fe_{ox}). (d) ratios of Fe in citrate/ascorbate to ammonium
814 oxalate. For the ridge, slope, and valley sites, n = 20 for each bar, and for the palm, palo colorado,
815 and elfin sites, n = 5 for each bar.

816

817 Figure 3: Pairwise relationships between soil C concentrations and biogeochemical variables
818 described in Table 2. Total n = 149 for each scatterplot, with 119 samples from the lower
819 montane and 30 from the montane sites; two outliers with Fe(II) concentrations > 10 mg g^{-1} are
820 not shown. As a heuristic, we report R^2 and statistical significance for each scatterplot,
821 acknowledging an overestimate of R^2 due to the spatial structure of our data: Al_{ca} ($R^2 = 0.35$, $p <$
822 0.0001); Al_{ox} ($R^2 = 0.29$, $p < 0.0001$); Al_{HCl} ($R^2 = 0.31$, $p < 0.0001$); $Fe(II)_{HCl}/Fe_{HCl}$ ($R^2 =$ 0.47,
823 $p < 0.0001$); Fe_{ca} ($R^2 = 0.01$, $p = 0.29$); Fe_{ox} ($R^2 = 0.18$, $p < 0.0001$); $Fe(III)_{HCl}$ ($R^2 = 0.01$; $p =$

824 0.86); $Fe_{cd\text{-}ca}$ ($R^2 = 0.22$, $p < 0.0001$); clay ($R^2 = 0.14$, $p < 0.0001$); sand ($R^2 = 0.10$, $p = 0.10$); silt

825 ($R^2 = 0.07$, $p < 0.001$); total fine roots ($R^2 = 0.61$, $p < 0.0001$).

826

827

828

829

830

831

832

833

834

835

836

837

838

839

840

841 Figure 1:

Figure 2:

859

860

861

862

863

864

865

866

867

868

869

870

871

872

873

874

875 Figure 3:

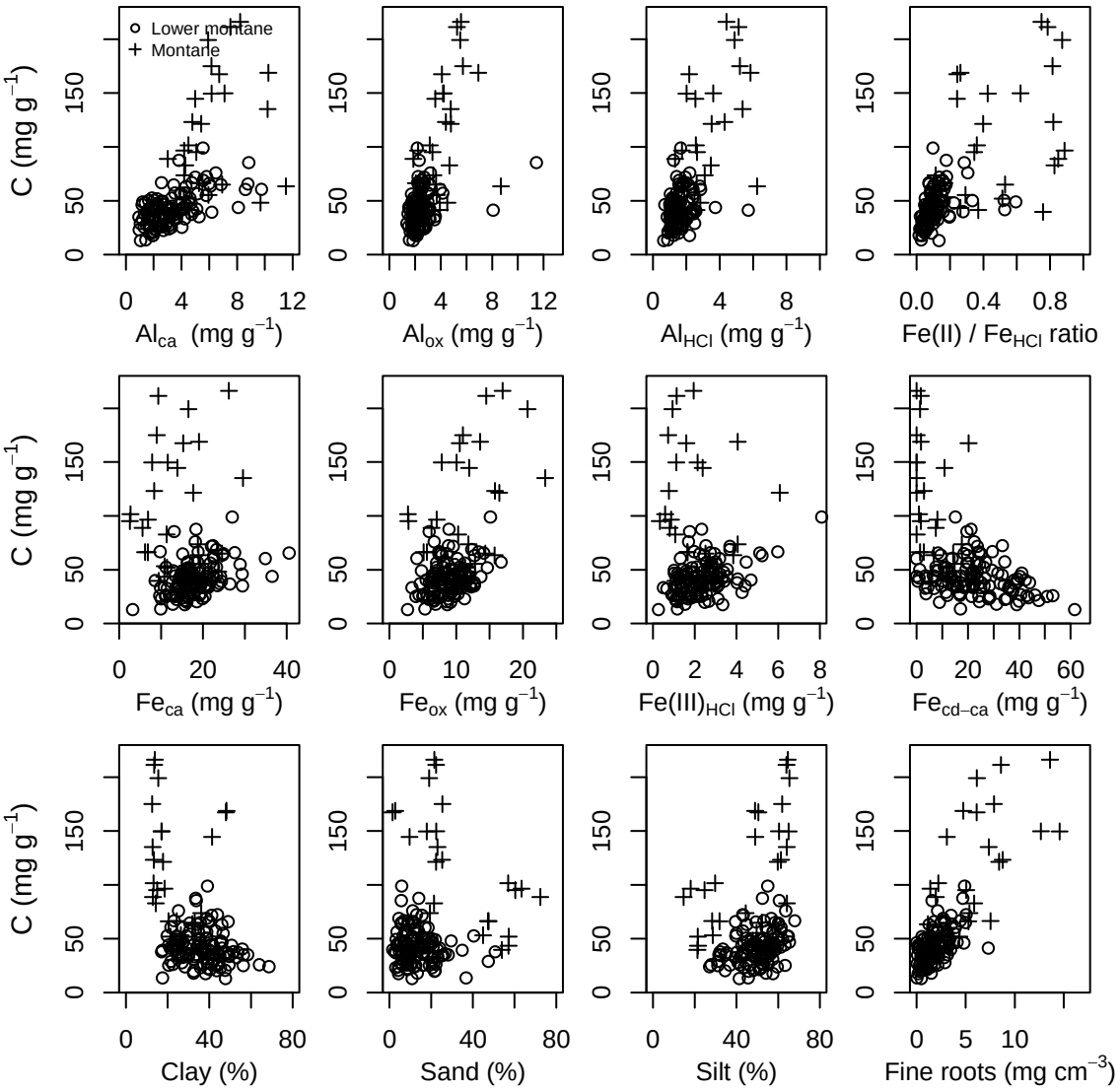

876

Supplementary Material

Supplemental Table 1: Pearson correlation coefficients between site means of C concentrations and biogeochemical covariates (n = 6 sites). Significant correlations are shown in bold face, where the number of asterisks denotes significance at $p < 0.05$, 0.01, 0.001, or 0.0001, respectively. See Table 2 for variable abbreviations. All units are mg g^{-1} except for C stocks and fine roots, which are reported in mg cm^{-3}.

	C	C stock	Al_{ca}	Fe_{ca}	Fe_{ox}	Fe(II)	$Fe(III)_{HCl}$	Fe_{cd}	Fe_{cd-ca}	O_2	Fe(II)/ Fe_{HCl}	Total roots	Live roots	Dead roots	Bulk density
C	1														
C stock	0.95	1													
Al_{ca}	0.73	0.52	1												
Fe_{ca}	-0.3	-0.41	0.07	1											
Fe_{ox}	0.74	0.6	0.63	0.26	1										
Fe(II)	**0.94****	**0.98*****	0.53	-0.55	0.51	1									
$Fe(III)_{HCl}$	-0.28	-0.46	0.26	**0.93****	0.26	-0.54	1								
Fe_{cd}	-0.71	-0.76	-0.25	0.75	-0.35	**-0.86***	0.67	1							
Fe_{cd-ca}	-0.74	-0.75	-0.32	0.53	-0.53	**-0.83***	0.45	**0.96****	1						
Fe(II)/Fe_{HCl}	**0.92****	0.95	0.53	-0.61	0.47	**0.99*****	-0.57	**-0.69***	**-0.85***	1					
O_2	-0.59	-0.56	-0.22	0.67	-0.44	-0.66	0.56	**0.90***	**0.87***	-0.7	1				
Total roots	**0.99*****	**0.99*****	0.65	-0.33	0.66	**0.96****	-0.36	-0.70	-0.71	-0.53	**0.93****	1			
Live roots	**0.86***	0.69	**0.96****	-0.19	0.63	0.73	-0.01	-0.50	-0.54	-0.45	0.74	0.79	1		
Dead roots	**0.93*****	**0.99*****	0.47	-0.35	0.60	**0.94****	-0.45	-0.70	-0.69	-0.50	**0.91***	**0.97*****	0.63	1	
Bulk density	-0.78	-0.58	**-0.96****	0.09	-0.66	-0.63	-0.14	0.47	0.56	0.45	-0.65	-0.68	**-0.97****	-0.50	1

Supplemental Table 2: Multiple comparisons among site means of soil C and other covariates stratified by depth interval. Sites with different letters significantly differ according to Tukey's honestly significant difference test. Differences among sites were assessed within a given depth interval for each variable.

Variable	Depth	Ridge	Slope	Valley	Palm	Palo colorado	Elfin
Soil C concentration	0 - 10 cm	a	ab	b	cd	abc	d
	10 -20 cm	ab	a	a	bc	c	d
Soil C stock	0 - 10 cm	a	a	a	a	a	b
	10 -20 cm	a	a	a	ab	b	c
Bulk density	0 - 10 cm	a	a	b	c	ab	ac
	10 -20 cm	a	a	a	a	a	a
$Fe(II)_{HCl}$	0 - 10 cm	b	a	ab	abc	abc	c
	10 -20 cm	b	a	ab	b	abc	c
$Fe(III)_{HCl}$	0 - 10 cm	a	a	a	a	a	a
	10 -20 cm	b	a	ab	ab	a	ab
$Fe(II)/Fe_{HCl}$	0 - 10 cm	a	a	a	a	ab	b
	10 -20 cm	a	a	a	ab	bc	c
Fe_{cd-ca}	0 - 10 cm	c	a	b	bc	bd	d
	10 -20 cm	a	a	b	b	bc	c
Fe_{ca}	0 - 10 cm	b	a	a	ab	c	a
	10 -20 cm	b	a	a	ab	c	ac
Fe_{ox}	0 - 10 cm	ab	a	b	c	ab	c
	10 -20 cm	ab	a	b	c	ab	abc
Al_{ca}	0 - 10 cm	ac	a	b	ac	a	c
	10 -20 cm	ac	a	b	ac	c	c

Supplemental Table 3: Linear mixed-effects models of soil C concentrations incorporating potential predictors listed in Table 2, where variables were eliminated by stepwise backwards elimination from the full model using t tests when $p > 0.05$. Standardized regression parameters (SE) were estimated using REML and are analogous to Pearson's r. Significance of fixed effects is indicated by asterisks where *, **, ***, and **** denote $p < 0.05$, 0.01, 0.001, and 0.0001, respectively. Separate models were fit for the lower montane and overall datasets. Pseudo-R^2 values represent the proportion of the total model variance (fixed effects, random effects, and residuals) explained by the fixed effects. Models included random effects for sites and plots to account for spatial correlation.

Variable	Parameter estimate (SE)	Variable	Parameter estimate (SE)
Lower montane		**Lower montane + montane**	
Depth	-0.52 (0.08)****	Al_{ca}	0.33 (0.05)****
Al_{ca}	0.40 (0.09)***	Depth	-0.30 (0.07)****
Fe_{ox}	0.31 (0.07)****	Total fine roots	0.26 (0.05)****
Fe_{ca}	-0.27 (0.07)***	$Fe(II)/Fe_{HCl}$	0.25 (0.05)****
$Fe(II)/Fe_{HCl}$	0.24 (0.05)****	Al_{ca} x $Fe(II)/Fe_{HCl}$	0.23 (0.04)****
Total fine roots	0.22 (0.05)***	Fe_{ox}	0.20 (0.04)****
$Fe(III)_{HCl}$	0.22 (0.06)***	Fe_{ca}	-0.16 (0.05)**
Al_{ca} x $Fe(II)/Fe_{HCl}$	0.13 (0.05)**		
Pseudo-R^2	0.77	*Pseudo-R^2*	*0.84*

Supplemental Table 4: Linear mixed-effects models of soil C stocks incorporating potential predictors listed in Table 2, where variables were eliminated by stepwise backwards elimination from the full model using t tests when $p > 0.05$. Standardized regression parameters (SE) were estimated using REML and are analogous to Pearson's r. Significance of fixed effects is indicated by asterisks where *, **, ***, and **** denote $p < 0.05$, 0.01, 0.001, and 0.0001, respectively. Separate models were fit for the lower montane and overall datasets. Pseudo-R^2 values represent the proportion of the total model variance (fixed effects, random effects, and residuals) explained by the fixed effects. Models included random effects for sites and plots to account for spatial correlation.

Variable	Parameter estimate (SE)	Variable	Parameter estimate (SE)
Lower montane		**Lower montane + montane**	
Fe_{ox}	0.50 (0.11)****	$Fe(II)/Fe_{HCl}$	0.37 (0.06)****
depth	-0.39 (0.13)**	Fe_{ox}	0.24 (0.07)***
Fe_{ca}	-0.33 (0.12)**	$Fe(II)/Fe_{HCl} \times Al_{ca}$	0.21 (0.06)***
Al_{ca}	0.31 (0.13)*	Al_{ca}	0.24 (0.07)***
		Fe_{ca}	-0.20 (0.07)**
Pseudo-R^2	*0.23*	*Pseudo-R^2*	*0.63*

Supplemental Figure 1:

Soil Fe(II) concentrations in the lower montane forest soils by topographic position and depth. Data from three different sampling campaigns (June 2011, Feb 2012, May 2012) on one catena were combined here. (a) box and whisker plots with outliers shown as dots. (b) data with outliers removed; means with different letters were significantly different.

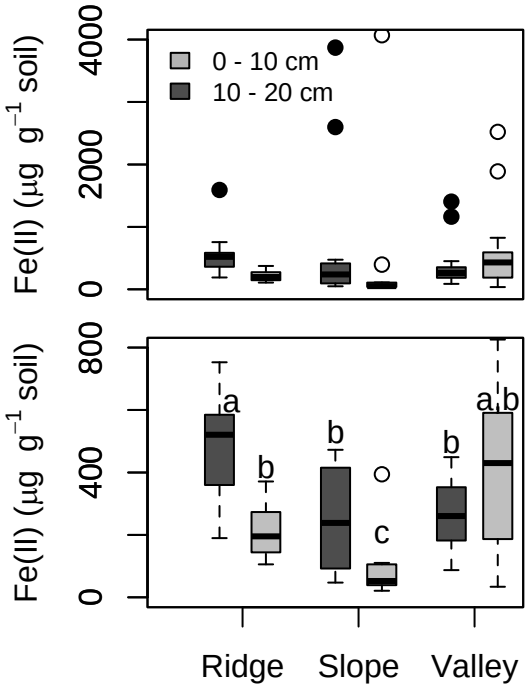

Supplemental Figure 2: Pairwise relationships between soil C stocks (mg cm^{-3}) and biogeochemical variables described in Table 2. Total n = 149 for each scatterplot, with 119 samples from the lower montane and 30 from the montane sites. Two outliers with Fe(II) concentrations > 10 mg g^{-1} are not shown. As a heuristic, we report R^2 and statistical significance for each scatterplot, acknowledging an overestimate of R^2 due to the spatial structure of our data: Al_{ca} ($R^2 = 0.15$, $p < 0.0001$); Al_{ox} ($R^2 = 0.19$, $p < 0.0001$); Al_{HCl} ($R^2 = 0.21$, $p < 0.0001$); $Fe(II)_{HCl}/Fe_{HCl}$ ($R^2 = 0.53$, $p < 0.0001$); Fe_{ca} ($R^2 = 0.04$, $p = 0.02$); Fe_{ox} ($R^2 = 0.13$, $p < 0.0001$);

$Fe(III)_{HCl}$ ($R^2 = 0.01$; $p = 0.37$); $Fe_{cd\text{-}ca}$ ($R^2 = 0.17$, $p < 0.0001$); clay ($R^2 = 0.19$, $p < 0.0001$); sand ($R^2 = 0.06$, $p = 0.003$); silt ($R^2 = 0.05$, $p = 0.006$); total fine roots ($R^2 = 0.40$, $p < 0.0001$).